

# Thermodynamic modeling of direct internal reforming solid oxide fuel cells operating with syngas

C. Ozgur Colpan<sup>a</sup>, Ibrahim Dincer<sup>b,\*</sup>, Feridun Hamdullahpur<sup>a</sup>

<sup>a</sup>Mechanical and Aerospace Engineering Department, Carleton University, 1125 Colonel By Drive, Ottawa, Ont., Canada K1S 5B6

<sup>b</sup>Faculty of Engineering and Applied Science, University of Ontario Institute of Technology, 2000 Simcoe Street North, Oshawa, Ont., Canada L1H 7L7

Received 17 June 2006; received in revised form 30 September 2006; accepted 28 October 2006

Available online 26 December 2006

## Abstract

In this paper a direct internal reforming solid oxide fuel cell (DIR-SOFC) is modeled thermodynamically from the energy point of view. Syngas produced from a gasification process is selected as a fuel for the SOFC. The modeling consists of several steps. First, equilibrium gas composition at the fuel channel exit is derived in terms mass flow rate of fuel inlet, fuel utilization ratio, recirculation ratio and extents of steam reforming and water–gas shift reaction. Second, air utilization ratio is determined according to the cooling necessity of the cell. Finally, terminal voltage, power output and electrical efficiency of the cell are calculated. Then, the model is validated with experimental data taken from the literature. The methodology proposed is applied to an intermediate temperature, anode-supported planar SOFC operating with a typical gas produced from a pyrolysis process. For parametric analysis, the effects of recirculation ratio and fuel utilization ratio are investigated. The results show that recirculation ratio does not have a significant effect for low current density conditions. At higher current densities, increasing the recirculation ratio decreases the power output and electrical efficiency of the cell. The results also show that the selection of the fuel utilization ratio is very critical. High fuel utilization ratio conditions result in low power output and air utilization ratio but higher electrical efficiency of the cell.

© 2006 International Association for Hydrogen Energy. Published by Elsevier Ltd. All rights reserved.

**Keywords:** Hydrogen; Solid oxide fuel cell; Internal reforming; Syngas; Thermodynamics; Model

## 1. Introduction

Solid oxide fuel cell (SOFC) is a solid state energy conversion device that contains an oxide ion-conducting electrolyte made from a ceramic material and operates at temperatures from 500 to 1000 °C. The basic ideas and materials were proposed by Nernst and his colleagues at the end of the 19th century. A detailed history of SOFCs may be found in [1].

SOFCs may be classified according to their temperature level, cell and stack design and reforming type; which is shown in Table 1.

Some detailed descriptions of these different types of SOFCs, advantages and disadvantages of each type over another, etc. may be found in literature [1–4].

Unlike lower temperature fuel cells, a wider range of fuel may be used in SOFCs due to not having a carbonmonoxide poisoning problem and being capable of reforming the fuel inside the cell. There are many options for choosing the fuel of SOFCs. Among these fuel options, H<sub>2</sub> and CO are electrochemically oxidized at the anode. The remaining ones are reformed into H<sub>2</sub> and/or CO and then electrochemically reacted. Methane, higher hydrocarbons, methanol, ethanol, landfill gas, biomass produced gas, ammonia, hydrogen sulfide, etc. may be fuel options for SOFCs. Many studies, mainly investigating the thermodynamic feasibility of these fuels to be used in SOFCs, may be found in literature [5–11].

SOFCs have high operating temperatures which enable successful thermal integration with bottoming cycles. Most of the studies in the literature investigate the opportunities of integration of SOFCs with gas turbine cycles [12–14]. Integration of SOFCs with gasification cycles [15–17] is another promising option. There are a few studies searching the integration

\* Corresponding author.  
E-mail addresses: [cocolpan@connect.carleton.ca](mailto:cocolpan@connect.carleton.ca) (C.O. Colpan),  
[Ibrahim.Dincer@uoit.ca](mailto:Ibrahim.Dincer@uoit.ca) (I. Dincer),  
[feridun\\_hamdullahpur@carleton.ca](mailto:feridun_hamdullahpur@carleton.ca) (F. Hamdullahpur).

Nomenclature			
$a$	extent of steam reforming reaction for methane, mol/s	$T$	temperature, K
$A$	active surface area, $\text{cm}^2$	$U_F$	fuel utilization ratio
$b$	extent of water–gas shift reaction, mol/s	$U_{ox}$	air (oxidant) utilization ratio
$c$	extent of electrochemical reaction, mol/s	$V$	voltage, V
$D_{aeff}$	effective gaseous diffusivity through the anode, $\text{cm}^2/\text{s}$	$\dot{W}_{FC}$	power output of the cell, W
$D_{ceff}$	effective gaseous diffusivity through the cathode, $\text{cm}^2/\text{s}$	$x$	molar concentration
$F$	Faraday constant, C	<i>Greek letters</i>	
$\bar{h}$	specific molar enthalpy, J/mol	$\rho$	electrical resistivity of cell components, ohm cm
$\dot{H}$	enthalpy flow rate, W	$\eta_{el,cell}$	electrical efficiency of the fuel cell
$i$	current density, $\text{A}/\text{cm}^2$	$\Delta\bar{g}$	change in specific molar gibbs free energy, J/mol
$i_{oa}$	exchange current density of anode, $\text{A}/\text{cm}^2$	<i>Subscripts</i>	
$i_{oc}$	exchange current density of cathode, $\text{A}/\text{cm}^2$	a	anode
$i_{as}$	anode-limiting current density, $\text{A}/\text{cm}^2$	act	activation
$i_{cs}$	cathode-limiting current density, $\text{A}/\text{cm}^2$	c	cathode
$I$	current, A	conc	concentration
$K$	equilibrium constant	e	electrolyte
$L$	thickness of a cell component, $\mu\text{m}$	eq	equilibrium
LHV	lower heating value, J/mol	ohm	ohmic
$\dot{m}$	mass flow rate, g/s	r	steam reforming reaction for methane
$M$	molecular weight, g/mol	s	water gas shift reaction; solid structure
$\dot{N}$	molar flow rate, mol/s	N	Nernst
$r$	recirculation ratio	<i>Superscripts</i>	
$P$	pressure, bar	a	anode
$R$	universal gas constant, J/mol K	c	cathode
		o	standard state

of renewable systems with SOFC. For example, Ntziachristos et al. [18] have studied the integration of a wind turbine with a SOFC (or PEM). More recently Hussain et al. [19–21] have conducted some leading studies on the multi-component and multi-dimensional modeling of SOFCs.

Two key points for thermodynamic modeling of SOFCs are determining the exit gas composition and thermal management. There are different approaches for calculating the exit gas

Table 1  
Classification of solid oxide fuel cells

Classification criteria	Types
Temperature level	1. Low temperature SOFC (LT-SOFC) (500–650 °C) 2. Intermediate temperature SOFC (IT-SOFC) (650–800 °C) 3. High temperature SOFC (HT-SOFC) (800–1000 °C)
Cell and stack design	1. Planar SOFC (Flat-planar and radial-planar design) 2. Tubular SOFC (Tubular and micro-tubular design) 3. Monolithic SOFC
Reforming	1. External reforming 2. Direct internal reforming SOFC (DIR-SOFC) 3. Indirect internal reforming (IIR-SOFC)

composition of the anode section of a SOFC in literature. A simple approach to calculate the SOFC effluent composition is given for a SOFC operating with 100% methane which is assumed to be completely reformed within the fuel cell in the fuel cell handbook by EGG [22]. The moisture required for the reforming is supplied by internal recirculation. In their approach, first, an intermediate solution is found by taking into account the combined fuel cell and steam reforming reaction for the part of the fuel that is utilized, and the steam reforming reaction for the part of the fuel that is not utilized. Then, the true exit gas composition is determined by considering the effect of the water–gas shift equilibrium. According to the approach of Achenbach and Riensche [23], steam reforming of methane reaction is kinetically controlled. An equation is proposed for the reforming kinetics in the form of the Arrhenius-type independence of the  $\text{H}_2\text{O}$  partial pressure and proportional to the  $\text{CH}_4$  partial pressure. On the other hand, in many studies [7,24,25], the steam reforming and water–gas shift reactions are considered in equilibrium, and, according to the reforming type, electrochemical reaction may or may not occur simultaneously with these reactions. In most of these studies, it is considered that hydrogen is the gas that is electrochemically oxidized since the CO oxidation rates are much lower than hydrogen, and CO is converted into  $\text{H}_2$  by water–gas shift reaction.

Thermal management of SOFCs is important due to operating the fuel cell safely, and thermodynamically and economically more efficient. In a SOFC operating with a gas mixture containing hydrocarbon, the heat is generated inside a SOFC due to electrochemical reaction, polarizations and water–gas shift reaction. Some of the heat generated is used by steam reforming reaction. The utilization of the remaining heat may be used in several ways: Yoshida and Iwai [26] have considered a SOFC system having the same inlet and outlet temperatures. In this system, the excess heat is utilized by a combustor which is positioned in close thermal contact with SOFC. It is also possible to operate the SOFC within a distinct temperature range. However, high temperature gradients are not desirable within a SOFC. So, maximum temperature difference between fuel cell inlet and exit becomes a design criterion. The cooling of the fuel cell is provided by using excess air at the cathode inlet. On the other hand, it is also important to maintain a uniform temperature gradient along the cell in minimizing the stresses in cell components [1]. Since the stresses are developed due to mismatch in coefficients of thermal expansions when there is a temperature difference between the fuel cell and the environment, the system should be insulated.

The primary purpose of this study is to develop a model for direct internal reforming SOFC (DIR-SOFC) taking into account the effect of recirculation ratio of the anode exit gas which is important especially for supplying water for initiating the chemical reactions and preventing carbon deposition. In addition, a method for calculating the air utilization ratio is developed.

## 2. Thermodynamic model

### 2.1. Operation principle

A unit cell is shown in Fig. 1. Syngas mixes with recirculated gas mixture and enters the fuel channel. Steam reforming of methane, water–gas shift and electrochemical reactions occur simultaneously at the anode. The gas mixture exiting the fuel channel has, generally, high water content. So, some portion of it may be recirculated since the chemical reactions need water as reactant. The oxidant, taken as air in this study, enters from the air channel. The oxygen molecules in the air react with the electrons, which are produced at the anode and cycled via

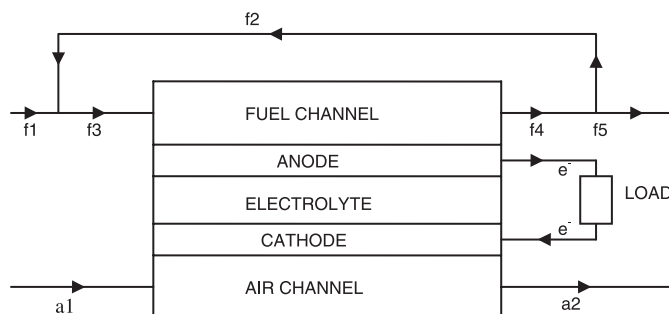


Fig. 1. Schematic of the DIR-SOFC.

the load. Oxide ions are produced at the cathode and they diffuse to the anode through the electrolyte. The gas mixture, having less oxygen content than the air entering, exits the air channel. Electric current is produced by the flow of electrons and it effectuates work on the load.

### 2.2. Assumptions

The following assumptions are made in the analysis:

- Syngas consists of the following gas species,  $i = \{\text{CH}_4, \text{CO}_2, \text{CO}, \text{H}_2\text{O}, \text{H}_2, \text{N}_2\}$ .
- Air consists of 79%  $\text{N}_2$  and 21%  $\text{O}_2$ ,  $j = \{\text{O}_2, \text{N}_2\}$ .
- Fuel cell operates at steady state.
- Gas mixture at the fuel channel exit is at chemical equilibrium.
- Pressure drops along the fuel cell are neglected.
- Temperature at the channel inlets is same ( $T_y = T_{f3} = T_{a1}$ ). Also, temperature at the channel exits is same ( $T_z = T_{f4} = T_{a2}$ ).
- Temperature of the solid structure is midway between the inlet and exit temperatures [27].
- Fuel cell is insulated which means that there is no heat interaction with environment.
- Only hydrogen is electrochemically reacted. CO is converted to  $\text{CO}_2$  and  $\text{H}_2$  by water–gas shift reaction.
- Contact resistances are ignored.
- Radiation transfer between solid structure and gas channels is ignored.

### 2.3. Input data

The volumetric gas composition at state ‘f1’ is chosen as a typical composition obtained from a pyrolysis process. In dry basis, the composition is as follows [28]: 21%  $\text{CH}_4$ , 40%  $\text{H}_2$ , 20%  $\text{CO}$ , 18%  $\text{CO}_2$ , 1%  $\text{N}_2$ . Other fixed input parameters are shown in Table 2. Among them, exchange current density depends on temperature and material. For the temperature used in this study and common SOFC materials, these values are obtained from literature [29]. Effective diffusivity through the

Table 2  
Input values that are fixed throughout the study

Input	Value
Temperature of the exit ( $T_z$ )	850 °C
Temperature difference between exit and inlet ( $\Delta T$ )	100 °C
Pressure of the cell ( $P_{\text{cell}}$ )	1 bar
Active surface area ( $A$ )	100 cm <sup>2</sup>
Exchange current density of anode ( $i_{\text{oa}}$ )	0.65 A/cm <sup>2</sup>
Exchange current density of cathode ( $i_{\text{oc}}$ )	0.25 A/cm <sup>2</sup>
Effective gaseous diffusivity through the anode ( $D_{\text{a,eff}}$ )	0.2 cm <sup>2</sup> /s
Effective gaseous diffusivity through the cathode ( $D_{\text{c,eff}}$ )	0.05 cm <sup>2</sup> /s
Thickness of anode ( $L_a$ )	500 μm
Thickness of electrolyte ( $L_e$ )	10 μm
Thickness of cathode ( $L_c$ )	50 μm

anode and cathode depends on material thickness and temperature. In this study, the cell is assumed to be an anode-supported cell and suitable values are chosen according to the data given by Singhal and Kendall [1].

Fuel utilization ratio, recirculation ratio and current density are chosen as varying input parameters. Current density is taken in a range from 0.1 to a close value to its maximum value. Recirculation ratio is taken as 0.1, 0.2 and 0.3. When the effect of fuel utilization is investigated, it is fixed at 0.2. Fuel utilization ratio is taken as 0.65, 0.75 and 0.85. When the effect of recirculation ratio is investigated, it is fixed at 0.85.

#### 2.4. Calculation of the equilibrium gas mixture composition at the fuel channel exit

Here, the first step is the calculation of the equilibrium gas composition at the fuel channel exit. We derive the equations in terms of total molar or mass flow rate of gas species at state 'f1'. Since, it is more convenient to adjust the mass flow rate for a system operator; the equations are given in terms of mass flow rate of state 'f1'. In this regard, the molar flow rate of gas species at state 'f1' may be given in terms of mass flow rate as follows:

$$\dot{N}_{f1}^i = x_{f1}^i \cdot \frac{\dot{m}_{f1}}{\sum x_{f1}^i \cdot M^i}, \quad (1)$$

Here, the states 'f2', 'f4' and 'f5' have the same molar compositions. The composition of gas species at these states is shown by  $x_{eq}^i$ . Then, the molar flow rate of gas species at the state 'f3' becomes

$$\dot{N}_{f3}^i = \dot{N}_{f1}^i + \dot{N}_{f2}^i = \dot{N}_{f1}^i + x_{eq}^i \cdot \dot{N}_{f2} = \dot{N}_{f1}^i + x_{eq}^i \cdot (r \cdot \dot{N}_{f4}). \quad (2)$$

The steam reforming reaction for methane, water–gas shift reaction and electrochemical reactions, which are shown in Eqs. (3)–(5), respectively, occur simultaneously at the cell as follows:



Let the extents of reactions shown in Eqs. (3)–(5) be  $a$ ,  $b$  and  $c$ , respectively. The molar flow rate of state 'f4' is given as

$$\dot{N}_{f4}^i = \dot{N}_{f3}^i + d^i, \quad \xrightarrow{\text{D?}} \quad (6)$$

where

$$d^{\text{CH}_4} = -a, \quad (6.1)$$

$$d^{\text{H}_2\text{O}} = -a - b + c, \quad (6.2)$$

$$d^{\text{CO}} = a - b, \quad (6.3)$$

$$d^{\text{CO}_2} = b, \quad (6.4)$$

$$d^{\text{H}_2} = 3a + b - c, \quad (6.5)$$

$$d^{\text{N}_2} = 0. \quad (6.6)$$

Here,  $c$  is also the molar flow rate of hydrogen utilized in the fuel cell which can also be defined as follows:

$$c = (\dot{N}_{f3}^{\text{H}_2} + 3a + b) \cdot U_F. \quad (7)$$

We obtain the following equation by summing molar flow rate of gas species at state 'f4' by using Eqs. (6)–(6.6) and combining with Eq. (2):

$$\dot{N}_{f3}^i = \dot{N}_{f1}^i + x_{eq}^i \cdot r \cdot (\dot{N}_{f3} + 2a). \quad (8)$$

The total molar flow rate of state 'f3' is given as

$$\dot{N}_{f3} = \frac{\dot{N}_{f1} + 2ar}{1 - r}. \quad (9)$$

Combining Eqs. (6)–(6.6), (8) and (9), the equilibrium molar gas composition at the fuel channel exit results in

$$x_{eq}^i = \frac{\dot{N}_{f4}^i}{\dot{N}_{f4}} = \frac{\dot{N}_{f1}^i + d^i}{\dot{N}_{f1} + 2a}. \quad (10)$$

The molar flow rate of hydrogen utilized,  $c$ , is redefined by combining Eqs. (6.5) and (7)–(10) as

$$c = \frac{(\dot{N}_{f1}^{\text{H}_2} + 3a + b) \cdot U_F}{1 - r + r \cdot U_F}. \quad (11)$$

Hence, using Eqs. (6)–(6.6), (10) and (11), the equilibrium gas composition at the fuel channel exit is found as

$$x_{eq}^{\text{CH}_4} = \frac{\dot{N}_{f1}^{\text{CH}_4} - a}{\dot{N}_{f1} + 2a}, \quad (12)$$

$$x_{eq}^{\text{H}_2} = \frac{(\dot{N}_{f1}^{\text{H}_2} + 3a + b)}{\dot{N}_{f1} + 2a} \cdot \left( \frac{(1 - r)(1 - U_F)}{1 - r + r \cdot U_F} \right), \quad (13)$$

$$x_{eq}^{\text{CO}} = \frac{\dot{N}_{f1}^{\text{CO}} + a - b}{\dot{N}_{f1} + 2a}, \quad (14)$$

$$x_{eq}^{\text{CO}_2} = \frac{\dot{N}_{f1}^{\text{CO}_2} + b}{\dot{N}_{f1} + 2a}, \quad (15)$$

$$x_{eq}^{\text{H}_2\text{O}} = \frac{\dot{N}_{f1}^{\text{H}_2\text{O}} + \left[ -a - b + (\dot{N}_{f1}^{\text{H}_2} + 3a + b) \cdot U_F / (1 - r + r \cdot U_F) \right]}{\dot{N}_{f1} + 2a}, \quad (16)$$

$$x_{eq}^{\text{N}_2} = \frac{\dot{N}_{f1}^{\text{N}_2}}{\dot{N}_{f1} + 2a}. \quad (17)$$

Here,  $a$ ,  $b$ , and molar flow rates of gas species at state 'f1' which are a function of  $\dot{m}_{f1}$  are unknown. So, we need three equations to be solved simultaneously to find  $a$ ,  $b$  and  $\dot{m}_{f1}$ . These are the chemical equilibrium equations corresponding to the steam reforming and water–gas shift reactions and the relation between electrical current and molar flow rate of hydrogen

utilized; which are shown in Eqs. (18)–(20), respectively.

$$K_r = \exp[-\Delta\bar{g}_r^\circ/RT_z] = \frac{(x_{\text{eq}}^{\text{CO}}) \cdot (x_{\text{eq}}^{\text{H}_2})^3}{(x_{\text{eq}}^{\text{H}_2\text{O}}) (x_{\text{eq}}^{\text{CH}_4})} \cdot \left(\frac{P}{P^\circ}\right)^2, \quad (18)$$

$$K_s = \exp[-\Delta\bar{g}_s^\circ/RT_z] = \frac{(x_{\text{eq}}^{\text{H}_2}) \cdot (x_{\text{eq}}^{\text{CO}_2})}{(x_{\text{eq}}^{\text{CO}}) (x_{\text{eq}}^{\text{H}_2\text{O}})}, \quad (19)$$

$$I = i \cdot A = 2 \cdot F \cdot c = 2 \cdot F \cdot \frac{(\dot{N}_{\text{fl}}^{\text{H}_2} + 3a + b) \cdot U_F}{1 - r + r \cdot U_F}. \quad (20)$$

The temperature dependent equilibrium constant is solved by the classical method in which the change in Gibbs free energy of the reactions is used. However, equilibrium constants for steam reforming and water–gas shift reactions may also be found by using a simple relation and equilibrium constant coefficients [30]. On the other hand, instead of doing calculations based on equilibrium constant, a more direct procedure which is based on minimization of the total Gibbs free energy may be used. In this method, it is not necessary to know the chemical reactions. Only, gas species that are present in the system, moles of species in the initial unreacted state, temperature and pressure should be known to calculate the equilibrium composition. Solution is found by using Lagrange multipliers. Further information on this may be found in Perry and Green [31].

### 2.5. Calculation of air utilization, terminal voltage, power output and cell efficiency

The cell analyzed in this study is assumed to be insulated, and the heat produced in the cell is carried away by sending excess air. Also, the maximum temperature difference is taken as 100 °C as to be determined as an input parameter to adjust the mass flow rate of air entering the air channel. Hence, the air utilization ratio is calculated according to the cooling necessity of the fuel cell.

The molar flow rates of gas species at the air channel inlet and exit are defined as follows:

$$\dot{N}_{\text{a1}}^{\text{O}_2} = \frac{c}{2 \cdot U_{\text{ox}}}, \quad (21)$$

$$\dot{N}_{\text{a1}}^{\text{N}_2} = \frac{c}{2 \cdot U_{\text{ox}}} \cdot \frac{79}{21} = \frac{79}{42} \cdot \frac{c}{U_{\text{ox}}}, \quad (22)$$

$$\dot{N}_{\text{a2}}^{\text{O}_2} = \frac{c}{2 \cdot U_{\text{ox}}} - \frac{c}{2} = \frac{c}{2} \left( \frac{1}{U_{\text{ox}}} - 1 \right), \quad (23)$$

$$\dot{N}_{\text{a2}}^{\text{N}_2} = \frac{79}{42} \cdot \frac{c}{U_{\text{ox}}}. \quad (24)$$

The gas composition at the air channel exit is calculated using the following:

$$x_{\text{a2}}^{\text{O}_2} = \frac{\dot{N}_{\text{a2}}^{\text{O}_2}}{\dot{N}_{\text{a2}}} = \frac{1 - U_{\text{ox}}}{100/21 - U_{\text{ox}}}, \quad (25)$$

$$x_{\text{a2}}^{\text{N}_2} = 1 - x_{\text{a2}}^{\text{O}_2}. \quad (26)$$

Here, the Nernst voltage is calculated as

$$V_N = \frac{-\Delta\bar{g}^\circ(T_z)}{2F} - \frac{RT_z}{2F} \cdot \ln \left( \frac{x_{\text{eq}}^{\text{H}_2\text{O}}}{x_{\text{eq}}^{\text{H}_2} \cdot \sqrt{x_{\text{a2}}^{\text{O}_2} \cdot P/P^\circ}} \right). \quad (27)$$

Here, three types of polarizations, e.g., ohmic, activation and concentration, are considered and calculated through Eqs. (28)–(32). The ohmic polarization is caused by the resistance to the flow of oxide ions through the electrolyte and resistance to the flow of electrons. The activation polarization is the voltage drop due to the sluggishness of reactions occurring at the electrode–electrolyte interfaces [1]. If we assume that charge transfer coefficient for anode and cathode is 0.5 and substitute this value in the Butler–Volmer equation, this equation takes the form as shown in Eq. (29) [29]. The concentration polarization is caused by the resistance to mass transport through the electrodes and interfaces [32]:

$$V_{\text{ohm}} = \left( R_{\text{contact}} + \sum_k \rho_k \cdot L_k \right) \cdot i \quad (28)$$

$$V_{\text{act}} = V_{\text{act,a}} + V_{\text{act,c}} = \frac{RT_s}{F} \cdot \sinh^{-1} \left( \frac{i}{2i_{\text{o,a}}} \right) + \frac{RT_s}{F} \cdot \sinh^{-1} \left( \frac{i}{2i_{\text{o,c}}} \right) \quad (29)$$

$$V_{\text{conc}} = V_{\text{conc}}^{\text{a}} + V_{\text{conc}}^{\text{c}} = \left[ -\frac{RT_z}{2F} \ln \left( 1 - \frac{i}{i_{\text{as}}} \right) + \frac{RT_z}{2F} \ln \left( 1 + \frac{p_{\text{f4}}^{\text{H}_2} \cdot i}{p_{\text{f4}}^{\text{H}_2\text{O}} \cdot i_{\text{as}}} \right) \right] + \left[ -\frac{RT_z}{4F} \ln \left( 1 - \frac{i}{i_{\text{cs}}} \right) \right], \quad (30)$$

where

$$i_{\text{as}} = \frac{2F \cdot p_{\text{f4}}^{\text{H}_2} \cdot D_{\text{aeff}}}{RT_z \cdot L_{\text{a}}}, \quad (31)$$

$$i_{\text{cs}} = \frac{4F \cdot p_{\text{a2}}^{\text{O}_2} \cdot D_{\text{ceff}}}{((P - p_{\text{a2}}^{\text{O}_2})/P) \cdot RT_z \cdot L_{\text{c}}}. \quad (32)$$

The electrical resistivity of cell components,  $\rho$ , is the inverse of electrical conductivities. The formulations for electrical conductivities of cell components, as a function of temperature of solid structure, for common SOFC materials are given by Bossel [30]. The terminal voltage and power output of the cell are given by

$$V = V_N - V_{\text{ohm}} - V_{\text{act}} - V_{\text{con}}, \quad (33)$$

$$\dot{W}_{\text{FC}} = I \cdot V. \quad (34)$$

Here, the enthalpy flow rate of state ‘f1’ is calculated using an energy balance around the control volume enclosing the junction point by Eq. (35). The temperature of this state is then found by iteration:

$$\dot{H}_{\text{f1}} = \sum \dot{N}_{\text{f1}}^i \cdot \bar{h}^i(T_x) = \sum \dot{N}_{\text{f3}}^i \cdot \bar{h}^i(T_y) - \sum \dot{N}_{\text{f2}}^i \cdot \bar{h}^i(T_z). \quad (35)$$

For the insulated fuel cell, the energy balance around the control volume enclosing the fuel cell is written as

$$\sum \dot{N}_{fl}^i \cdot \bar{h}^i + \sum \dot{N}_{al}^j \cdot \bar{h}^j = \dot{W}_{FC} + \sum \dot{N}_{f5}^i \cdot \bar{h}^i + \sum \dot{N}_{a2}^j \cdot \bar{h}^j. \quad (36)$$

Here, the air utilization is calculated through an iterative solution method using Eq. (36). After obtaining air utilization by iteration, terminal voltage and power output of the cell is found using Eqs. (33) and (34).

Finally, the electrical efficiency of the cell is calculated as

$$\eta_{el,cell} = \frac{\dot{W}_{FC}}{\dot{N}_{fl} \cdot LHV}. \quad (37)$$

The flowchart of the MathCAD program used for the model is shown in Fig. 2.

## 2.6. Validation of the model

The experimental works for DIR-SOFCs lack in the literature in terms of usage of different fuels and information about the input parameters used for the experiment. In the present model, taking the channel inlet and exit temperatures different, taking the fuel cell as insulated, and using a syngas make it difficult to find data for comparison purpose from literature. However, experimental data with methane as fuel presented by Tao et al. [33] are used for comparison with the model results as given in Table 3. It is seen that the difference is in the range of  $\pm 12\%$  for the voltage and  $\pm 8\%$  for the power output which sort of validates the model. This difference is mainly due to the assumptions considered in the model and the comparison.

## 3. Results and discussion

The model developed in this study may be summarized as follows: In the first part of the model; using principles of thermodynamics, mathematical manipulations and definitions of some fuel cell related parameters such as fuel utilization ratio; fuel channel equilibrium exit gas composition is derived in terms of extents of chemical reactions and molar flow rate of gas species at the fuel channel inlet. Then using chemical equilibrium equations and the relation between the electric current and the molar flow rate of hydrogen that is utilized, exit gas composition of the fuel channel exit is found. In the second part of the model, air utilization ratio which measures the amount of excess air that should be sent to the air channel to carry away the unutilized heat in the fuel cell is calculated for an insulated fuel cell and a controlled fuel inlet and exit gas temperature. So, air channel inlet and exit gas composition, Nernst voltage, polarizations and work output of the fuel cell are derived in terms of air utilization ratio. Using the first law of thermodynamics for the control volume enclosing the fuel cell, this ratio is calculated. After finding this ratio, fuel cell output parameters; such as cell voltage, work output of the cell and electrical efficiency of the cell are found. The procedure is repeated for each current density, recirculation ratio and fuel utilization ratio.

In this study, the formulations to find the exit gas composition of the anode section are derived for a gas mixture including water vapor as fuel. If there is enough amount of water vapor in the initial gas mixture, it may not be necessary to recirculate the anode exit gas stream. However, if we consider a more general case in which, for example, a dry gas mixture is used as the fuel, recirculation is necessary for a DIR-SOFC to initiate the steam reforming and water–gas shift reactions. Hydrogen produced by these reactions is utilized by the electrochemical reaction simultaneously, and more amount of water vapor than the amount of that necessary for initiating the reactions is produced. This study is simplified by considering the cell as a whole which may be regarded as a zero-dimensional modeling approach. Due to this fact, it is not possible to track the change of gas composition along the cell. An improved method may be dividing the cell into several sections to analyze the change of gas composition along the cell. If such a method is applied, the effect of initial water vapor amount may be seen more clearly.

In literature, it may be seen that different input and output parameters are used in different thermodynamic models of SOFCs. For example, fuel utilization may be considered as an input parameter in one study and an output parameter in another study. In this study, input parameters are determined according to the recirculation and thermal management considerations. Due to this, mass flow rate and temperature of the inlet fuel are considered as output. These parameters may be adjusted by the system operator accordingly.

The recirculation ratio adjusts the steam to carbon ratio entering the anode section. In many studies in literature, it is seen that carbon deposition problem is related with this ratio. However, this problem is not considered in this study; rather, its effect on system performance is investigated. High recirculation ratios increase the system's complexity which is generally undesirable. The effect of this ratio on output parameters is shown in Fig. 3. It may be observed from the figures that its effect is not very significant for low current densities. For high current densities, as recirculation ratio increases, mass flow rate of fuel, air utilization ratio, terminal voltage, power output, and electrical efficiency of the cell decrease. Having a lower air utilization ratio means higher mass flow rate of air entering from the cathode sections; which in turn increases the cost of the system. However, the mass flow rate of fuel decreases in this condition which decreases the operation cost.

It is known that there is always some unused hydrogen and that the degree of the utilization of hydrogen is determined by the fuel utilization ratio. Fig. 4 shows the effect of fuel utilization ratio on output parameters. Unlike recirculation ratio, its effect is more significant. It may be observed from the figures that a wider range of current density may be selected for lower fuel utilization ratios. As fuel utilization ratio increases, mass flow rate of fuel, air utilization ratio, terminal voltage, and power output of the cell decrease; whereas electrical efficiency of the cell increases. It may be considered controversial to have low power output and high electrical efficiency at the same time. This is due to the fact that less mass flow rate of fuel is



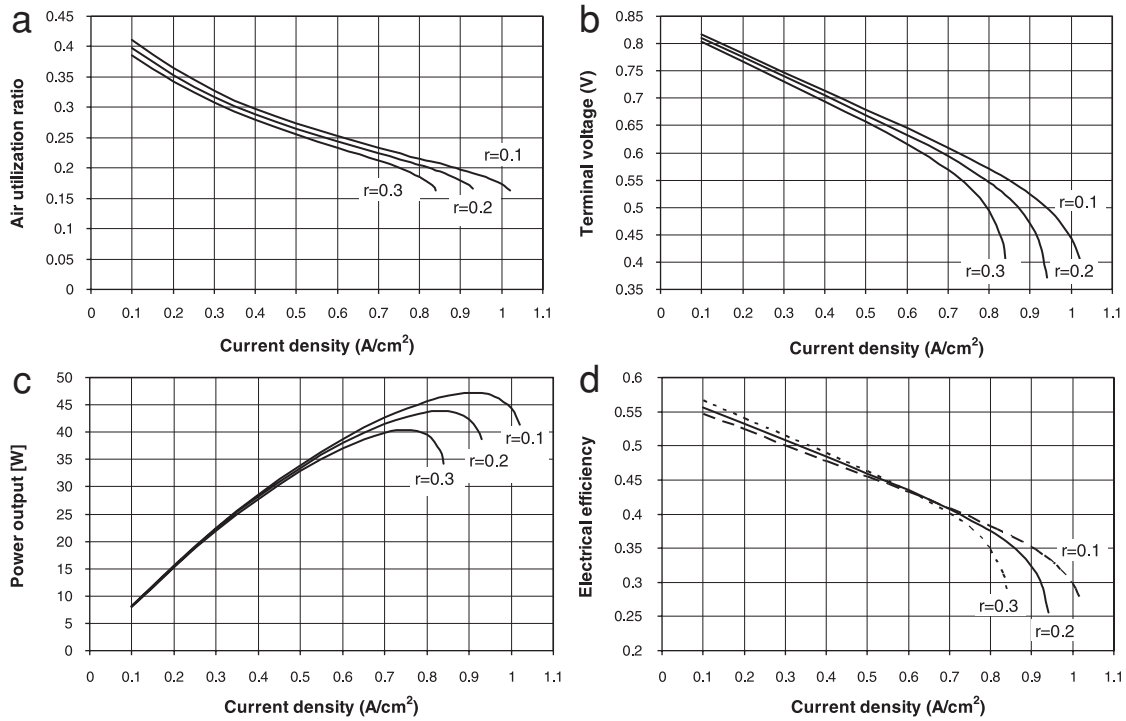


Fig. 3. Effect of recirculation ratio and current density on (a) air utilization ratio; (b) terminal voltage; (c) power output; (d) electrical efficiency; for fuel utilization ratio of 0.85.

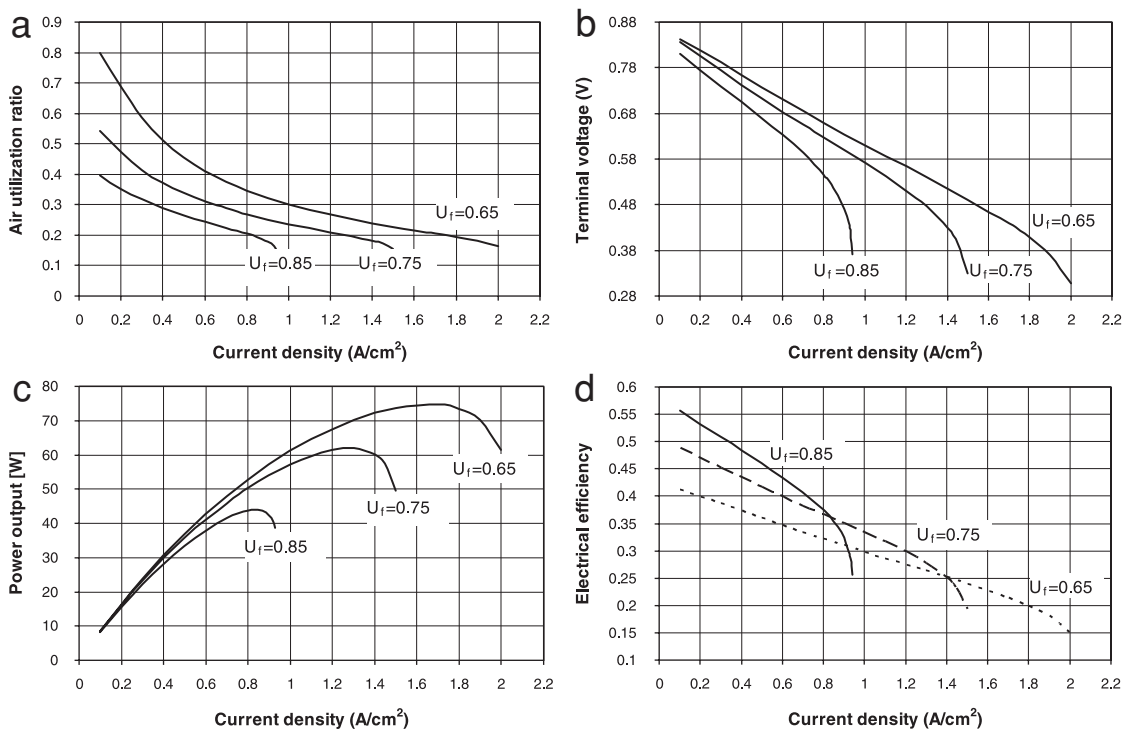


Fig. 4. Effect of fuel utilization ratio and current density on (a) air utilization ratio; (b) terminal voltage; (c) power output; (d) electrical efficiency; for recirculation ratio of 0.2.

needed for higher fuel utilization ratios. Hence, it is seen that increasing this ratio improves the system thermodynamically and decreases the cost of fuel; but also increases the cost of the air flow entering the cathode section.

#### 4. Conclusions

In this study, a DIR-SOFC operating with syngas has been modeled thermodynamically. The recirculation of the anode

exit gas stream is taken into account in the model to obtain a formulation valid for gas mixtures containing different gas compositions. The effect of recirculation ratio and fuel utilization ratio is also investigated. The conditions that are thermodynamically effective and economically effective are identified and discussed. Future study will concentrate on the thermo-economic optimization of the DIR-SOFC and enhancement of the present model including the carbon deposition using the finite control volume method.

## Acknowledgments

The financial and technical support of an Ontario Premier's Research Excellence Award, the Natural Sciences and Engineering Research Council of Canada, Carleton University and University of Ontario and Institute of Technology is gratefully acknowledged.

## References

- [1] Singhal SC, Kendall K. High temperature solid oxide fuel cells—fundamentals design and applications. UK: Elsevier; 2002.
- [2] Singhal SC. Science and technology of solid oxide fuel cells. MRS Bulletin 2000;25(3):16–21.
- [3] Singhal SC. Solid oxide fuel cells for stationary, mobile, and military applications. Solid State Ionics 2002;152–153:405–10.
- [4] Larminie J, Dicks A. Fuel cell systems explained. 2nd ed., England: Wiley; 2003.
- [5] Assabumrungrat S, Pavarajarn V, Charojrochkul S, Laosiripojana N. Thermodynamic analysis for a solid oxide fuel cell with direct internal reforming fueled by ethanol. Chem Eng Sci 2004;59:6015–20.
- [6] Assabumrungrat S, Laosiripojana N, Pavarajarn V, Sangtongkitcharoen W, Tangjitmatee A, Praserttham P. Thermodynamic analysis of carbon formation in a solid oxide fuel cell with a direct internal reformer fuelled by methanol. J Power Sources 2005;139:55–60.
- [7] Lu Y, Schaefer L. A solid oxide fuel cell system fed with hydrogen sulfide and natural gas. J Power Sources 2004;135:184–91.
- [8] Van herle J, Marechal F, Leuenberger S, Favrat D. Energy balance model of a SOFC cogenerator operated with biogas. J Power Sources 2003;118:375–83.
- [9] Wojcik A, Middleton H, Damopoulos I, Van herle J. Ammonia as a fuel in solid oxide fuel cells. J Power Sources 2003;118:342–8.
- [10] Yi Y, Rao AD, Brouwer J, Samuelsen GS. Fuel flexibility study of an integrated 25 kW SOFC reformer system. J Power Sources 2005;144:67–76.
- [11] Yin Y, Zhu W, Xia C, Gao C, Meng G. Low-temperature SOFCs using biomass-produced gases as fuels. J Appl Electrochem 2004;34:1287–91.
- [12] Palsson J, Selimovic A, Sjunnesson L. Combined solid oxide fuel cell and gas turbine systems for efficient power and heat generation. J Power Sources 2000;86:442–8.
- [13] Winkler W, Lorenz H. The design of stationary and mobile solid oxide fuel cell—gas turbine systems. J Power Sources 2002;105:222–7.
- [14] Koyama M, Kraines S, Tanaka K, Wallace D, Yamada K, Komiyama H. Integrated model framework for the evaluation of an SOFC/GT system as a centralized power source. Int J Energy Res 2004;28:13–30.
- [15] Kivisaari T, Björnbohm P, Sylwan C, Jacquinet B, Jansen D, de Groot A. The feasibility of a coal gasifier combined with a high-temperature fuel cell. Chem Eng J 2004;100:167–80.
- [16] Kuchonthara P, Bhattacharya S, Tsutsumi A. Combination of thermochemical recuperative coal gasification cycle and fuel cell for power generation. Fuel 2005;84:1019–21.
- [17] Ghosh S, De S. Energy analysis of a cogeneration plant using coal gasification and solid oxide fuel cell. Energy 2006;31:345–63.
- [18] Ntziachristos L, Kouridis C, Samaras Z, Pattas K. A wind-power fuel-cell hybrid system study on the non-interconnected Aegean islands grid. Renewable Energy 2005;30:1471–87.
- [19] Hussain MM, Li X, Dincer I. Multi-component mathematical model of solid oxide fuel cell anode. Int J Energy Res 2005;29(7):1083–101.
- [20] Hussain MM, Dincer I, Li X. Mathematical modeling of transport phenomena in porous SOFC anodes. Int J Thermal Sci 2007;46(1):48–56.
- [21] Hussain MM, Li X, Dincer I. Mathematical modeling of planar solid oxide fuel cells. J Power Sources 2006;161(2):1012–22.
- [22] EG&G. Fuel cell handbook. 7th ed. West Virginia: U.S Department of Energy; 2004.
- [23] Achenbach E, Riensche E. Methane/steam reforming kinetics for solid oxide fuel cells. J. Power Sources 1994;52:283–8.
- [24] Massardo AF, Lubelli F. Internal reforming solid oxide fuel cell-gas turbine combined cycles (IRSOFC-GT): Part A-cell model and cycle thermodynamic analysis. Trans ASME-A—Eng For Gas Turbines Power 2000;122(1):27–35.
- [25] Ghosh S, De S. Thermodynamic performance study of an integrated gasification fuel cell combined cycle—an energy analysis. Proc Inst of Mech Eng-A 2003;217(2):137–47.
- [26] Yoshida H, Iwai H, Thermal management in solid oxide fuel cell systems, In: Shah RK, Ishizuka M, Rudy TM, Wadekar W, Editors. Proceedings of fifth international conference on enhanced, compact and ultra-compact heat exchangers: science, engineering and technology, Engineering Conferences International, Hoboken, NJ, USA, 2005.
- [27] Omosun AO, Bauen A, Brandon NP, Adjiman CS, Hart D. Modelling system efficiencies and costs of two biomass-fuelled SOFC systems. J Power Sources 2004;131:96–106.
- [28] Bridgwater AV. The technical and economic feasibility of biomass gasification for power generation. Fuel 1995;74(5):631–53.
- [29] Chan SH, Low CF, Ding OL. Energy and exergy analysis of simple solid-oxide fuel-cell power systems. J Power Systems 2002;103:188–200.
- [30] Bossel UG. Final report on SOFC data facts and figures. Berne, CH: Swiss Federal Office of Energy; 1992.
- [31] Perry RH, Green OW. Perry's chemical engineers' handbook. 7th ed., McGraw-Hill: USA; 1997.
- [32] Kim J, Virkar AV, Fung K, Mehta K, Singhal SC. Polarization effects in intermediate temperature, anode-supported solid oxide fuel cells. J Electrochem Soc 1999;146(1):69–78.
- [33] Tao G, Armstrong T, Virkar A. Intermediate temperature solid oxide fuel cell (IT-SOFC) research and development activities at MSRI. In: Nineteenth annual ACERC&ICES conference. Utah; 2005.